Characterization of the Microsomal Cytochrome P450 2B4 O_2 Activation Intermediates by Cryoreduction and Electron Paramagnetic Resonance[†]

Roman Davydov,[‡] Reza Razeghifard,[§] Sang-Choul Im,[§] Lucy Waskell,*[,§] and Brian M. Hoffman*[,‡]

Department of Chemistry, Northwestern University, 2145 Sheridan Road, Tech K148, Evanston, Illinois 60208-3113, and Department of Anesthesiology, University of Michigan, and VA Medical Center, Ann Arbor, Michigan 48105

Received May 16, 2008; Revised Manuscript Received July 2, 2008

ABSTRACT: The oxy−ferrous complex of cytochrome P450 2B4 (2B4) has been prepared at −40 °C with and without bound substrate [butylated hydroxytoluene (BHT)] and radiolytically one-electron cryoreduced at 77 K. Electron paramagnetic resonance (EPR) shows that in both cases the observed product of cryoreduction is the hydroperoxo−ferriheme species, indicating that the microsomal P450 contains an efficient distal-pocket proton-delivery network. In the absence of substrate, two distinct hydroperoxo−ferriheme signals are observed, reflecting the presence of two major conformational substates in the oxy−ferrous precursor. Only one species is observed when BHT is bound, indicating a more ordered active site. BHT binding also changes the **g**-tensor components of the hydroperoxo−ferric 2B4 intermediate, indicating that the substrate modulates the properties of this intermediate. Step annealing the cryoreduced ternary 2B4 complex at ≥175 K causes the loss of hydroperoxo−ferric 2B4 and the parallel appearance of high-spin ferric 2B4; liquid chromatography−tandem mass spectroscopy (LC−MS/MS) analysis shows that in this process BHT is quantitatively converted to two products, hydroxymethyl BHT (**1**) and 3-hydroxy-*tert*-butyl BHT (**2**). This implies that the hydroperoxo−ferric 2B4 prepared by cryoreduction is catalytically active and that the high-spin state observed after annealing contains an enzyme-bound product of BHT monooxygenation. The ratio of products generated during cryoreduction and annealing (6.2/1) is significantly different from the ratio (2.5/1) at ambient temperature. These findings suggest that substrate is held more rigidly relative to the oxidizing species at low temperatures and/or that dissociation of FeOOH is inhibited at low temperature. As in experiments under ambient conditions, product formation is not observed with the inactive F429H 2B4 mutant.

Xenobiotic-metabolizing cytochromes P450 (P450)[1] from mammalian liver microsomes function by oxidizing fat-soluble compounds, thereby converting them to excretable water-soluble compounds. Mammalian membrane-bound cytochromes P450 are able to react with a large variety of structurally diverse compounds because they have flexible substrate-binding sites that accommodate structurally diverse substrates (*1–3*).

Monooxygenation reactions, such as those carried out by P450s, are discussed in terms of the following reaction pathway: (1) substrate binding to the ferric protein, (2) reduction of the substrate−protein complex to the ferroheme form, (3) binding of dioxygen, and (4) activation of the oxyferroheme by reduction with a second electron to form the peroxo intermediate [Fe(III)−[O_2^{2-}]] (Scheme 1). In principle, this species can itself react (*4, 5*) or accept a proton to form the hydroperoxo−ferric intermediate [Fe(III)−[OOH^-]], which in turn may either react or undergo proton-assisted heterolytic cleavage of the O−O bond to form Compound I (Cpd I), the oxo−Fe(IV) porphyrin π-cation radical (*6*). Which species is reactive depends on the active-site environment, as modulated by the substrate, and on the substrate reactivity (*7, 8*).

Recent cryoreduction EPR/ENDOR studies have characterized the elusive steps of the monooxygenase cycle subsequent to step 4 for the bacterial cytochrome P450cam (*9*) and in doing so confirmed the generally held view (*4, 10*) that Cpd I is the reactive species for this enzyme with camphor as the substrate. However, analogous studies showed that methylene camphor also is oxidized by the hydroperoxo−ferric intermediate (*7, 8*).

In these experiments, 77 K γ-irradiation of the ternary complex of ferrous P450cam with O_2 and camphor in frozen solution generates a trapped one-electron reduced oxy−P450 intermediate (step 4) whose rhombic EPR signal is characteristic of a hydropero−ferriheme species. During step annealing at temperatures of ≥180 K, the cryotrapped intermediate converts to a state in which the hydroxycamphor monooxygenation product is coordinated to the ferriheme through its hydroxyl. ENDOR studies showed that this process indeed occurs via Cpd I, although this intermediate was not directly detected in these experiments, probably because of its high reactivity and low steady-state concentra-

[†] This work has been supported by the National Institutes of Health (Grant HL 13531 to B.M.H. and Grant GM35533 and VA grants to L.W.).

* To whom correspondence should be addressed. B.M.H.: phone, (847) 491-3104; fax, (847) 491-7713; e-mail, bmh@northwestern.edu. L.W.: phone, (734) 845-5858; fax, (734) 845-3096; e-mail, waskell@umich.edu.

[‡] Northwestern University.

[§] University of Michigan and VA Medical Center.

[1] Abbreviations: P450, cytochrome P450; 2B4, cytochrome P450 2B4; BHT, butylated hydroxytoluene; BP, benzphetamine; EPR, electron paramagnetic resonance.

10.1021/bi800926x CCC: $40.75
Published on Web 08/13/2008

Scheme 1

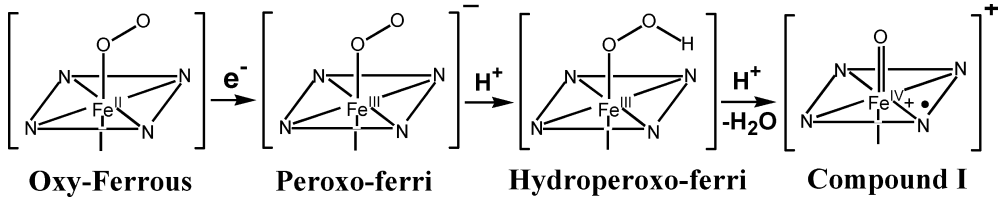

tion. In analogous crystallographic experiments with the ternary complex of camphor bound to oxy P450cam at >100 K, the hydroperoxy−ferric P450 intermediates were not detected but a state with an Fe−O bond and an average bond length of ∼1.67 Å was revealed, and the authors considered the possibility that this might even contain Compound I (*11*).

This cryoreduction study of the intermediates in the monooxygenase cycle of cytochrome P450 2B4 (2B4) is important as it is the first for a mammalian enzyme and is particularly interesting because the study of this enzyme helped initiate the idea that each of the three activated forms, peroxo, hydroperoxo, and Cpd I, might be a reactive species under the proper circumstances (*12, 13*). Application of cryoreduction methods to 2B4 has been hindered by two difficulties. One is rapid autoxidation of the oxyferro−2B4 complex, which makes it difficult to prepare this complex at high concentrations (0.5−1 mM) for study. We here report that the oxy−2B4 complex prepared in 60% glycerol solutions in the presence of substrate at −40 °C and pH 8.0 offers relief from this difficulty. The second is that although the widely used model substrate benzphetamine (BP, Figure 1) binds tightly at ambient temperatures, the affinity of 2B4 for BP decreases upon cooling, to the extent that freezing at −40 °C or below does not trap the BP complex. This problem is overcome through use of butylated hydroxytoluene (BHT, Figure 1) as a substrate, as we have found that it remains bound to 2B4 at low temperatures in the presence of 0.3 M NaCl (R. Razeghifard and L. Waskell, unpublished observations). These two approaches enable us to report the EPR study of an intermediate in the catalytic cycle of a mammalian cytochrome P450, the hydroperoxy−ferric 2B4 formed during cryoreduction of the oxy−2B4 and ternary oxy−P4502B4·BHT complexes, and to present an EPR investigation of its properties and step annealing measurements of its reactivity. The catalytic competence of the cryogenerated, one-electron reduced oxy−2B4·BHT complex is established by the determination that products of BHT monooxygenation form quantitatively during the cryoreduction and annealing of the ternary complex with wild-type 2B4, but not with the noncatalytic 2B4(F429H) variant.

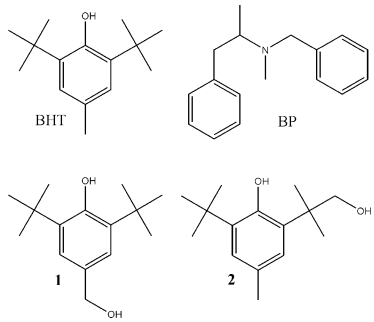

FIGURE 1: Cytochrome P450 2B4 substrates, BHT and BP, and products, hydroxymethyl BHT (**1**) and 3-hydroxy-*tert*-butyl BHT (**2**).

MATERIALS AND METHODS

Chemicals. All organic solvents, BHT, hydroxymethyl BHT (**1** in Figure 1), BP (Figure 1), NADPH, and sodium dithionite were from Sigma-Aldrich (St. Louis, MO). 3-Hydroxy-*tert*-butyl BHT (**2**) was a generous gift from J. Thompson (School of Pharmacy, University of Colorado, Boulder, CO). High-purity glycerol was purchased from Roche Diagnostics (Indianapolis, IN). O_2 and CO were obtained from Cryogenic Gas (Detroit, MI). The Vivaspin-2 concentrator (MWCO 30000) was from Biosciences (St. Louis, MO).

Full-length wild type 2B4 was expressed in *Escherichia coli* and purified as previously described (*14*). The concentration of 2B4 was determined using an extinction coefficient ($\Delta\varepsilon_{450-490}$) of 91 mM^{-1} cm^{-1} for the 2B4−CO complex (*14*). To prepare the oxy−2B4 complex, the protein was concentrated at 4 °C using a Vivaspin-2 concentrator (30000 MW cutoff) to 1 mM in a buffer consisting of 20% glycerol, 0.6 M NaCl, and 0.1 M Tris-HCl (pH 8) at room temperature. To 200 μL of the concentrated protein was added less than 1 μL of an ∼1 M stock solution of BP or BHT in methanol. Glycerol then was added to the P450−substrate complex to yield a final protein concentration of 0.5 mM P450, in 50 mM Tris-HCl (pH 8) at room temperature, 0.3 M NaCl, and 60% glycerol. The final concentration of BP in the sample was 2 mM, while the final BHT concentration was 0.5 or 2.0 mM. The 0.5 mM P450 solution was stored in liquid nitrogen until further use, at which time it was defrosted and placed in a glovebox at 4 °C overnight to remove the oxygen. An aliquot of a standardized solution of sodium dithionite was added to reduce the ferric P450 by one electron, using a 10−20% excess of dithionite to remove possible residual O_2. The reduced protein was cooled to −40 °C in a dry ice/ethanol bath. Precooled O_2 was bubbled (5−10 min) through the protein solution and mixed into the viscous 60% glycerol solution to form the oxy−2B4 complex. The oxygen was precooled in a stainless steel coil immersed in a dry ice/ethanol bath at −70 °C. The oxy−P450−substrate complex content in the samples prepared in this way varied between 70 and 80% because part of the oxy−P450 complex underwent autoxidation to the ferric protein during sample preparation.

Irradiation of the frozen solutions of the oxy−2B4 complex at 77 K typically was performed for 20−25 h at a rate of 0.15 Mrad/h (total dose of ∼3 Mrad) using a Gammacell 220 ^{60}Co as described previously (*15*). We performed annealing at multiple temperatures over the range of 77−270 K by placing the EPR sample in a bath at the desired temperature [usually *n*-pentane (T < 180 K) or

methanol ($T > 175$ K) cooled with liquid nitrogen] for the desired time and then refreezing the sample in liquid nitrogen.

EPR Spectroscopy. X-Band continuous wave EPR spectra were recorded on a Bruker ESP 300 spectrometer equipped with an Oxford Instruments ESR 910 continuous He flow cryostat. The amount of hydroperoxo−ferric 2B4·BHT complex produced by cryoreduction was determined by comparing the EPR signal from this species to that of a 0.5 mM solution of substrate free low-spin ferric 2B4 as a standard. To decrease interference from radicals formed during the irradiation, the quantitations were performed on solutions that had first been annealed for 1 min at 175 K. The radical signal is greatly diminished in this step, while this is the highest temperature at which the hydroperoxo−ferric state does not react. Quantitations of multiple samples showed that a 3 Mrad dose at 77 K reduces approximately 40% of the oxy−2B4·BHT complex present, generating 0.14(3) mM hydroperoxo−ferric 2B4·BHT complex in the samples as prepared.

Product Analysis. The oxidation of BP to its N-demethylated metabolite, norbenzphetamine, was assessed by a LC−MS/MS assay as previously described (*14*). Quantification of the BHT oxygenation products, **1** (major product) and **2**, was performed via LC−MS/MS. For quantifying BHT metabolites, 100 μL of each EPR sample was spiked with 0.3 mM 2,4-di-*tert*-butyl phenol as the internal standard. The solution was saturated with NaCl and extracted twice with an equal volume of hexane. The two hexane phases were recovered, pooled, and dried under a stream of nitrogen gas before being redissolved in 600 μL of acetonitrile. LC−MS/MS analysis was performed on a ThermoFinnegan (San Jose, CA) TSQ Quantum Ultra AM mass spectrometer. BHT and its metabolites were separated on a 4.6 mm × 250 mm Luna column (Phenomenex) at a flow rate of 1.0 mL/min. Mobile phases were water (solvent A) and acetonitrile (solvent B). The HLPC running conditions were as follows: initial conditions of 60:40 (A:B) followed by three linear gradients from 40 to 70% B in 20 min and from 70 to 90% in 30 min and from 90 to 100% B in 10 min. The column was then returned to the initial conditions (60:40 A:B) in 1 min and reequilibrated for 9 min, resulting in a total run time of 70 min. Elution of **1**, **2**, internal standard, and BHT occurred at 18, 26, 29, and 37 min, respectively. Since under these experimental conditions they were easily deprotonated during electrospray ionization to form negative pseudomolecular ions, the negative ion mode was employed for detection.

RESULTS AND DISCUSSION

EPR of Ferric 2B4. We have studied the effect of the substrates and products on the EPR spectra of ferric 2B4 to characterize their binding to the protein, to generate reference spectra for assignment of ferric species in the EPR spectra of the irradiated samples of the oxy−2B4 complex, and to help in the identification of product complexes formed during cryoreduction and step annealing.

Resting-state ferric 2B4 contains a low-spin aquoferriheme whose rhombic EPR signal has $\mathbf{g} = [2.43, 2.25, 1.92]$ (Table 1), in agreement with previous studies (*16*). Optical spectroscopy shows that addition of saturating amounts of BP to a 2B4 solution at ambient temperature causes the majority of enzyme to convert to the five-coordinate, high-spin, substrate-bound form. However, the amount of the high-spin form decreases upon cooling, and it is mostly gone by −40 °C (*17*); once the sample has frozen, one primarily observes the low-spin aquoferri-heme EPR signal, with only ∼5−10% of the enzyme in the high-spin BP-bound form ($\mathbf{g} = [8.1, 3.5, \sim 2]$). It is likely that this reflects a virtually complete loss of substrate during the cooling−freezing process, although the same phenomena would be observed if BP shifts to a more distant position in the heme pocket, thereby permitting the retention of Fe-bound water. For the sake of simplicity, we mostly discuss solutions frozen in the presence of BP as containing "substrate-free" enzyme to distinguish them from solutions without the addition of any substrate.

Table 1: g Values for Low-Spin Ferric Cytochrome P450 2B4 and Its Complexes with Substrates[a]

substrate	g_1	g_2	g_3
none	2.43	2.25	1.91
BHT	2.43	2.24	1.92
	2.39	2.24	1.97
1			
minor	2.54	2.26	1.87
major	2.42	2.24	1.92
minor	2.39	2.24	1.97

[a] The sample preparation and measurement of EPR spectra are described in Materials and Methods.

Under ambient conditions (25 °C), BHT binds stoichiometrically to ferric 2B4 in 60% glycerol and 0.3 M NaCl, and it remains ≅90% bound at −40 °C. Frozen solutions (77 K) of ferric 2B4 in the presence of BHT show a majority high-spin signal from BHT-bound enzyme, with the same g values as for the BP-bound form. In addition, there are signals from two minority, unidentified low-spin species. The g values of one of these minority species are close to those for substrate-free ferric 2B4 (Table 1), while those of the other, with $\mathbf{g} = [2.39, 2.24, 1.97]$, resemble very much those for substrate-bound P450cam in which camphor was proposed to act as the sixth ligand to the ferric heme (*18*). This suggests that at low temperatures the hydroxyl group of BHT can coordinate to the ferric iron of 2B4.

Under ambient conditions (25 °C, pH 7.4, 0.3 M NaCl), optical spectroscopy shows that in the presence of an excess of **1**, the major product of BHT metabolism, 2B4, is ∼64% high-spin and ∼36% low-spin. The former presumably has **1** bound in the heme pocket, while the latter does not. However, the EPR spectrum of a frozen solution of ferri-2B4 in the presence of **1** shows a largely low-spin signal resembling substrate-free protein (Table 1), suggesting that **1**, like BP, either is lost from the heme pocket or moves within it during freezing. In addition, there is a new minor rhombic low-spin EPR signal that has $\mathbf{g} = [2.54, 2.26, 1.87]$ that may be attributed to enzyme with the hydroxymethyl group of **1** coordinated to the ferric heme iron, in addition to one minor low-spin signal and one minor high-spin signal (Table 1).

EPR of the Cryoreduced Oxy−2B4·BHT Complex and the Oxy−2B4 Complex (2B4 + BP). As reported previously, the oxy−2B4 complex is much less stable than that of the oxy−P450cam complex (*19*). The lifetime of the oxy−2B4 complex is significantly increased by substrate binding, increases in pH, and lower temperatures (*19*). To optimize conditions for preparation of samples, we carried out kinetic studies on the decay of the oxy−P450 complex with and

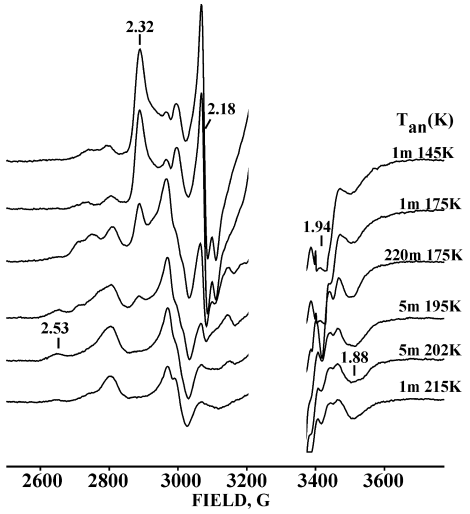

FIGURE 2: EPR spectra of cryoreduced ternary oxy−2B4·BHT complex annealed at the indicated temperatures for the specified times in minutes (m). Conditions: microwave frequency, 9.361 GHz; 30 K; modulation amplitude, 10 G.

Table 2: *g* Values for the Hydroperoxo−Ferri-2B4 Complex Formed by Cryoreduction of the Oxy−2B4 Complex, with and without Substrate[a]

substrate	species	g_1	g_2	g_3
none[b]	**A**	2.29	2.16	1.94
	B	2.34	2.19	nd
BHT		2.32	2.18	1.94

[a] Sample preparation and measurement of EPR spectra are described in Materials and Methods. [b] Prepared in the presence of BP; see the text.

without substrate as a function of pH and temperature using stopped-flow spectrophotometry. These results indicate that autoxidation of 0.5 mM oxy−2B4 complex to the ferric form is minimized if BP (2−3 mM) or stoichiometric BHT is present in a solution containing 60% glycerol, 50 mM Tris buffer (pH 8.0−8.2), and 0.3 M NaCl (measured at 25 °C) and the sample is oxygenated at −40 °C. As noted above, the frozen sample prepared with BHT is largely the ternary complex, and it contained ∼20−30% ferric form. Whether BP is indeed excluded from the active site or merely adopts an alternate conformation within it, the presence of the BP nonetheless serves to assist the trapping of the oxy complex; even so, the samples contain ∼20−30% ferric form. In the absence of any substrate, the amount of ferri-2B4 in a frozen sample is significantly higher.

Oxy−2B4·BHT Ternary Complex. Figure 2 presents the EPR spectrum of the oxy−2B4·BHT ternary complex after exposure to γ-irradiation at 77 K. The main signal from the cryoreduced ternary complex has **g** = [2.32, 2.176, ∼1.94]. These values, in particular a g_1 of ≥2.27, show that 77 K cryoreduction has produced the hydroperoxo−ferriheme state (*9*) (Table 2). At a dose of 3 Mrad, the yield of this species is ∼40% of the total ternary complex (∼0.14 mM).

It has been shown that the primary product of 77 K cryoradiolytic reduction of oxy hemoproteins is the peroxo−ferriheme, which then accepts a proton to generate the hydroperoxo state (*20*). The heme-containing monooxygenases studied previously, P450cam (*9*) and heme oxygenase (HO) (*21*), each contain an efficient distal-pocket proton-delivery network that can supply this proton even at 77 K; indeed, proton delivery in heme oxygenase has been seen at liquid helium temperatures (*22*). In contrast, the D251N

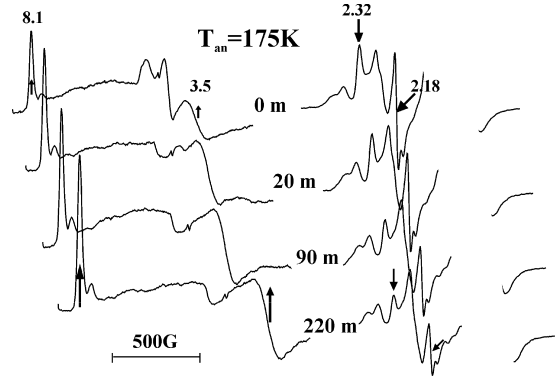

FIGURE 3: EPR spectra of the cryoreduced ternary oxy−2B4·BHT complex, showing loss of the hydroperoxoferric signal and growth of the high-spin ferric signal during annealing at 175 K for indicated times (minutes, m). Spectra other than that taken at time zero are arbitrarily offset to higher field to permit a better perspective on the annealing behavior. Measurement temperatures: low-field spectra, 8 K; high-field spectra, 30 K. Conditions: microwave frequency, 9.365 GHz; modulation amplitude, 10 G.

mutation of P450cam perturbs this proton-delivery network to the extent that protonation of the cryogenerated peroxo−ferric intermediate occurs only at a much higher temperature (<170 K) (*9*). The observation that 77 K cryoreduction of the oxy−2B4 complex generates the hydroperoxo−ferric heme indicates that this mammalian enzyme also has an efficient proton-delivery network. We surmise that for oxy−monooxygenase complexes that exhibit such a network, reduction under physiological conditions commonly will involve proton-coupled electron transfer to form the hydroperoxy−ferric species.

Figure 2 shows EPR spectra taken during annealing of the cryoreduced oxy−2B4·BHT ternary complex at successively higher temperatures. During this process, the hydroperoxo−ferric 2B4·BHT intermediate decays at approximately ≥175 K. Figure 3 shows that the decay of the hydroperoxo−ferric 2B4·BHT complex during annealing at 175 K is accompanied by a parallel increase in the magnitude of the high-spin ferri-2B4 signal, **g** = [8,1, 3.5, ∼2] (Figure 3), seen as the minority (10%) signal from a solution of ferri-2B4 frozen in the presence of the product, **1**. We propose that this product state likewise contains **1** that remains trapped in the distal pocket of the frozen sample, without coordination to the ferriheme. Thus, it is proposed to be analogous to the high-spin form with bound **1** that is observed by optical spectroscopy at room temperature.

This supposition is supported by the product analysis presented below, and by the fact that high-spin ferriheme is not formed when the cryoreduced substrate-free oxy−2B4 complex is annealed (see below). The loss of the hydroperoxo−ferriheme intermediate and the appearance of the high-spin product state have approximately the same half-times (not shown), consistent either with direct reaction of the hydroperoxo−ferric species or with formation of Cpd I, which reacts promptly to form product without accumulating. We further propose that the weak ferriheme signal with a g_1 of 2.54 that appears during subsequent annealing at 195−205 K reflects a relaxation of the heme pocket to the equilibrium product complex of **1**, discussed above. This relaxation competes with dissociation of the product complex, which can occur in glycerol solutions at these low temperatures

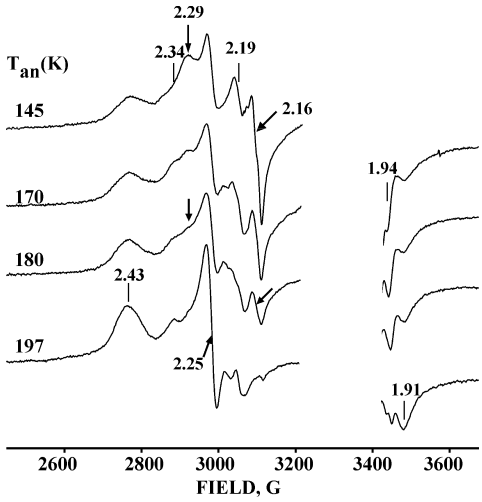

FIGURE 4: EPR spectra of the cryoreduced binary oxy−2B4 complex (prepared in the presence of BP) annealed at the indicated temperatures. The conditions are like those described in the legend of Figure 2.

(*23*), and ultimately, the $g_1 = 2.54$ signal disappears with further annealing.

Substrate-Free Oxy−2B4 Complex. Figure 4 presents the EPR spectrum of the binary oxy−2B4 complex (prepared in the presence of 2 mM BP) after exposure to γ-irradiation at 77 K. Although the spectrum is complicated by signals from the ferriheme formed by autoxidation (Table 1), it nonetheless clearly reveals two EPR signals from the hydroperoxo−ferri-2B4 complex generated by cryoreduction of the oxy−2B4 complex, a major conformer (**A**) with **g** = [2.29, 2.16, 1.942] and minor conformer (**B**) with **g** = [∼2.34, 2.19, nd] (Table 2), in addition to a decreased low-spin ferric 2B4 signal (in the irradiated samples, ∼40% of available ferric 2B4 contamination is reduced to the EPR-silent ferrous state). As conformational rearrangements are quenched at 77 K, the observation of two signals in the product of cryoreduction means that the active site of the parent oxy−2B4 complex adopts at least two different major conformational substates. This is likely the explanation for the biphasic kinetics of autoxidation of the oxy−2B4 complex at ambient temperature (*24*).

The *g* values of both the cryogenerated hydroperoxo−ferric centers of substrate-free 2B4 are different from that of the BHT-bound enzyme, which indicates that the active-site structure is modulated by the substrate, as reported previously for cytochrome P450cam (*7*). However, the observation of the hydroperoxo−ferriheme center after 77 K cryoreduction means that in the majority conformation(s) the 2B4 proton-delivery pathway remains effective in the substrate-free enzyme.

At a dose of 3 Mrad, the yield of the cryoreduced species is ∼40% of the total oxy−P450 complex (∼0.14 mM). Interestingly, the yield of the species increases only slightly at a dose of 7−8 Mrad. This is probably due to further cryoreduction of cryogenerated hydroperoxo species at doses above 7−8 Mrad which occurs with the cryogenerated hydroperoxo−ferric HO intermediate (*25*).

During progressive annealing from 145 to 170 K, the intensity of signal **A** ($g = 2.29, 2.16$) decreases while that of signal **B** ($g = 2.34, 2.19$) increases (Figure 4), suggesting a possible conversion of A to B; both signals then decay during annealing at 180 K (Figure 4). This process is accompanied by an increase in the magnitude of the resting, low-spin aquo−ferriheme signal ($g = 2.43, 2.25, 1.93$) (Figure 4), in contrast to the appearance of the high-spin product signal upon annealing the hydroperoxo−ferriheme center formed in the ternary complex.

Table 3: Concentrations of Products (millimolar) Generated by Step Annealing the Cryogenerated Hydroperoxo−Ferri-2B4·BHT Complex

protein−substrate complex	[Fe-OOH][a]	[**1**][b]	[**2**][b]	[**1**] + [**2**][b]
oxy−2B4·BHT (1:8)[c]	0.14(3)	0.101	0.016	0.117
oxy−2B4·BHT (1:1)[c]	0.14(3)	0.101	0.016	0.117
oxy−2B4(F429H)·BHT (1:8)[c]	0.16(3)	0.007	nd	0.007

[a] Hydroperoxo−ferri-2B4·BHT complex generated with a 3 Mrad radiation dose, as determined by EPR spin quantitations. Numbers in parentheses are uncertainties in the last digit. [b] Product formation as measured by the LC−MS/MS assay. [c] Total enzyme, 0.5 mM; initial concentration of oxy−2B4 complex, 0.4 mM. Numbers in parentheses are the molar ratios of oxy−2B4 to BHT.

Product Formation following Cryoreduction and under Steady-State Conditions. To correlate the cryoreduction measurements of microsomal oxy−2B4·BHT complexes with processes that occur under ambient conditions, and using physiological redox partners, product formation was assessed following annealing of the cryoreduced ternary complex.

Table 3 presents data showing that the cryogenerated hydroperoxo−ferric 2B4·BHT complex is catalytically competent. Application of the liquid chromatography−mass spectrometry assay to cryoreduced samples subsequent to annealing reveals the formation of **1** and **2**, consistent with the products of BHT oxygenation as observed during catalysis in solution at 25 °C under steady-state conditions. The absence of these metabolites in control experiments in which the ferri-2B4·BHT complex was irradiated excludes the possibility that product was generated during warming, through reaction of ferric 2B4 with radiolytically generated H_2O_2 (*26*). Likewise, cryoreduction and annealing of oxy-2B4 prepared in the presence of BP do not form the product norbenzphetamine, further substantiating our conclusion based on spectroscopic data that BP does not bind to the oxy−2B4 complex at low temperatures. This negative result is noteworthy because at ambient temperatures, BP oxidation occurs with a rate constant that is ≅38% faster than that of BHT (*14*).

According to our estimates, the maximal concentration of the cryogenerated hydroperoxo intermediate is 0.14 ± 0.3 mM, whereas the LC−MS/MS assay showed the formation of ∼0.12 mM BHT metabolites (Table 3). We thus infer that the hydroperoxo−ferric 2B4·BHT species prepared by cryoreduction of the ternary oxy−2B4·BHT complex quantitatively converts BHT to **1** (major product) and **2** (minor product) in a reaction that is characterized by relatively strong coupling. The product distribution and coupling for BHT hydroxylation in the cryoreduction experiment differ somewhat from those obtained under steady-state conditions at 30 °C with NADPH cytochrome P450 reductase as the electron donor. Conversion of BHT into product by the cryogenerated hydroperoxo intermediate is characterized by stronger "coupling", ∼80% versus 32%, and a higher molar ratio of **1** to **2** (6.2) as opposed to a ratio of 2.5 measured at ambient temperature and with the physiological electron donor. These differences suggest that at these lower temperatures, the substrate is held more rigidly in the proximity

of the active oxidizing species, and/or that the low temperature inhibits side product formation and dissociation of the protonated FeOOH species that result in uncoupling.

Table 3 presents a further example of the agreement between ambient and cryoreduction conditions. When the oxyferrous, BHT-bound 2B4(F429H) variant is cryoreduced, the hydroperoxo species accumulates to the same extent as with the wild-type enzyme. The subsequent annealing of the hydroperoxo intermediate of the F429H mutant, however, exhibits a markedly decreased level of product formation. Only ≅4% of the hydroperoxo−ferric 2B4(F429H) intermediate forms product compared to ≅80% with the native protein. This result agrees with our finding under ambient conditions, where the 2B4(F429H) mutant has only ≅5% of the activity of the native protein.

In conclusion, our results demonstrate the feasibility and the promise of cryoreduction/EPR and ENDOR spectroscopy in the study of the dioxygen activation by mammalian cytochromes P450. Cryoreduction at 77 K generates the hydroperoxo−ferriheme intermediate, which oxygenates substrate with efficiency comparable to that seen during steady-state catalysis under ambient conditions. Future cryoreduction ENDOR experiments with isotope-labeled substrates, carried out with oxy−2B4 samples prepared by a rapid freeze-quench method, combined with step annealing kinetic measurements conducted in H_2O/D_2O, will be carried out to determine the nature of active species in the catalytic cycle (hydroperoxo−ferri-P450 or compound I) and the details of the rate-limiting catalytic step(s).

ACKNOWLEDGMENT

We thank Professor Howard Halpern (University of Chicago, Chicago, IL) for providing access to the Gammacell irradiator. We thank Drs. Kate Noon and Yoichi Osawa from the Biomedical Mass Spectrometry Facility at the University of Michigan for assistance with the LC−MS/MS assay.

REFERENCES

1. Johnson, E. F., and Stout, C. D. (2005) Structural diversity of human xenobiotic-metabolizing cytochrome P450 monooxygenases. *Biochem. Biophys. Res. Commun. 338*, 331–336.
2. Zhao, Y., and Halpert, J. R. (2007) Structure-function analysis of cytochromes P 450 2B. *Biochim. Biophys. Acta 1770*, 402–412.
3. Scott, E. E., White, M. A., He, Y. A., Johnson, E. F., Stout, C. D., and Halpert, J. R. (2004) Structure of Mammalian Cytochrome P450 2B4 Complexed with 4-(4-Chlorophenyl)imidazole at 1.9-Å Resolution: Insight into the Range of P450 Conformations and the Coordination of Redox Partner Binding. *J. Biol. Chem. 279*, 27294–27301.
4. Ortiz de Montellano, P. R., and De Voss, J. J. (2002) Oxidizing Species in the Mechanism of Cytochrome P450. *Nat. Prod. Rep. 19*, 477–493.
5. Zhu, Y., and Silverman, R. B. (2008) Revisiting Heme Mechanisms. A Perspective on the Mechanisms of Nitric Oxide Synthase (NOS), Heme Oxygenase (HO), and Cytochrome P450s (CYP450s). *Biochemistry 47*, 2231–2243.
6. Newcomb, M., Hollenberg, P. F., and Coon, M. J. (2002) Multiple mechanisms and multiple oxidants in P 450-catalyzed hydroxylations. *Arch. Biochem. Biophys. 409*, 72–79.
7. Davydov, R., Perera, R., Jin, S., Yang, T.-C., Bryson, T. A., Sono, M., Dawson, J. H., and Hoffman, B. M. (2005) Substrate Modulation of the Properties and Reactivity of the Oxy-Ferrous and Hydroperoxoferric Intermediates of Cytochrome P450cam as Shown by Cryoreduction- EPR/ENDOR Spectroscopy. *J. Am. Chem. Soc. 127*, 1403–1413.
8. Jin, S., Makris, T. M., Bryson, T. A., Sligar, S. G., and Dawson, J. H. (2003) Epoxidation of Olefins by Hydroperoxo-Ferric Cytochrome P450. *J. Am. Chem. Soc. 125*, 3406–3407.
9. Davydov, R., Makris, T. M., Kofman, V., Werst, D. W., Sligar, S. G., and Hoffman, B. M. (2001) Hydroxylation of Camphor by Reduced oxy-Cytochrome P450cam: Mechanistic Implications of EPR and ENDOR of Catalytic Intermediates in Native and Mutant Enzymes. *J. Am. Chem. Soc. 123*, 1403–1415.
10. Hlavica, P. (2004) Models and mechanisms of O-O bond activation by cytochrome P450. A critical assessment of the potential role of multiple active intermediates in oxidative catalysis. *Eur. J. Biochem. 271*, 4335–4360.
11. Schlichting, I., Berendzen, J., Chu, K., Stock, A. M., Maves, S. A., Benson, D. E., Sweet, B. M., Ringe, D., Petsko, G. A., and Sligar, S. G. (2000) The catalytic pathway of cytochrome P450cam at atomic resolution. *Science 287*, 1615–1622.
12. Vaz, A. D. N., Pernecky, S. J., Raner, G. M., and Coon, M. J. (1996) Peroxo-iron and oxenoid-iron species as alternative oxygenating agents in cytochrome P450-catalyzed reactions: Switching by threonine-302 to alanine mutagenesis of cytochrome P450 2B4. *Proc. Natl. Acad. Sci. U.S.A. 93*, 4644–4648.
13. Coon, M. J. (2003) Multiple oxidants and multiple mechanisms in cytochrome P450 catalysis. *Biochem. Biophys. Res. Commun. 312*, 163–168.
14. Zhang, H., Im, S.-C., and Waskell, L. (2007) Cytochrome b5 Increases the Rate of Product Formation by Cytochrome P450 2B4 and Competes with Cytochrome P450 Reductase for a Binding Site on Cytochrome P450 2B4. *J. Biol. Chem. 282*, 29766–29776.
15. Davydov, R., Kofman, V., Nocek, J., Noble, R. W., Hui, H., and Hoffman, B. M. (2004) Conformational Substates of the Oxyheme Centers in α and β Subunits of Hemoglobin as Disclosed by EPR and ENDOR Studies of Cryoreduced Protein. *Biochemistry 43*, 6330–6338.
16. LeLean, J. E., Moon, N., Dunham, W. R., and Coon, M. J. (2000) EPR Spectrometry of Cytochrome P450 2B4: Effects of Mutations and Substrate Binding. *Biochem. Biophys. Res. Commun. 276*, 762–766.
17. Harris, D. L., Park, J.-Y., Gruenke, L., and Waskell, L. (2004) Theoretical study of the ligand-CYP2B4 complexes: Effect of structure on binding free energies and heme spin state. *Proteins: Struct., Funct., Bioinf. 55*, 895–914.
18. Lipscomb, J. D. (1980) Electron paramagnetic resonance detectable states of cytochrome P-450cam. *Biochemistry 19*, 3590–3599.
19. Bonfils, C., Debey, P., and Maurel, P. (1979) Highly-purified microsomal P-450: The oxyferro intermediate stabilized at low temperature. *Biochem. Biophys. Res. Commun. 88*, 1301–1307.
20. Davydov, R., Satterlee, J. D., Fujii, H., Sauer-Masarwa, A., Busch, D. H., and Hoffman, B. M. (2003) A Superoxo-Ferrous State in a Reduced Oxy-Ferrous Hemoprotein and Model Compounds. *J. Am. Chem. Soc. 125*, 16340–16346.
21. Davydov, R., Kofman, V., Fujii, H., Yoshida, T., Ikeda-Saito, M., and Hoffman, B. (2002) Catalytic Mechanism of Heme Oxygenase through EPR and ENDOR of Cryoreduced Oxy-Heme Oxygenase and its Asp140 Mutants. *J. Am. Chem. Soc. 124*, 1798–1808.
22. Davydov, R., Chemerisov, S., Werst, D. E., Rajh, T., Matsui, T., Ikeda-Saito, M., and Hoffman, B. M. (2004) Proton Transfer at Helium Temperatures during Dioxygen Activation by Heme Monooxygenases. *J. Am. Chem. Soc. 126*, 15960–15961.
23. Denisov, I. G., Makris, T. M., and Sligar, S. G. (2001) Cryotrapped reaction intermediates of cytochrome P450 studied by radiolytic reduction with phosphorus-32. *J. Biol. Chem. 276*, 11648–11652.
24. Zhang, H., Gruenke, L., Arscott, D., Shen, A., Kasper, C., Harris, D. L., Glavanovich, M., Johnson, R., and Waskell, L. (2003) Determination of the Rate of Reduction of Oxyferrous Cytochrome P450 2B4 by 5-Deazariboflavin Adenine Dinucleotide T491V Cytochrome P450 Reductase. *Biochemistry 42*, 11594–11603.
25. Garcia-Serres, R., Davydov, R. M., Matsui, T., Ikeda-Saito, M., Hoffman, B. M., and Huynh, B. H. (2007) Distinct Reaction Pathways Followed upon Reduction of Oxy-Heme Oxygenase and Oxy-Myoglobin as Characterized by Moessbauer Spectroscopy. *J. Am. Chem. Soc. 129*, 1402–1412.
26. Spinks, J. W. T., and Woods, R. J. (1990) *An Introduction to Radiation Chemistry*, 3rd ed., John Wiley & Sons, New York.

BI800926X